7.1.6 Determination of unstiffened element "effective width" using nonlinear finite element modeling

The "effective width" method provides an approximation to the complex non-uniform stress distribution in a thin buckled plate under compression. Initially presented in the 1930's by von Karman and extended to cold-formed steel members by Winter in the 1940's, the method accounts for the reduction in load-carrying capacity of a stiffened element (von Karman et al. 1932; Winter 1947). The inability of the center of the plate to carry compressive load is caused by out-of-plane deformations in the shape of the fundamental elastic buckling mode. These deformations reduce the axial stiffness, concentrating the compressive force at the edges of a plate. The ultimate load is reached when these edge stresses, carried by the "effective width", exceed the yield stress of the plate material. The "effective width" concept is the basis of most cold-formed steel design codes around the world today.

In this study, a nonlinear finite element model is employed to calculate the longitudinal stress distribution at failure for a stiffened element with and without a slotted hole. The distribution of stresses for both cases is compared, and the variation in effective width along the length of the stiffened element is determined. The stiffened element is modeled with the same loading and boundary conditions, dimensions, material properties, and solution controls as those used for the STAB2 model discussed in Section 7.1.3.4 and described in Table 7.1. The initial imperfection geometry corresponds to the fundamental elastic buckling mode of the plate without the hole as described in Figure 7.9. d_1/t=0.34 is used to scale the initial imperfection field of the

plate, which corresponds to a probability of occurrence of $P(\Delta<d_1)=0.50$ as discussed in Section 7.1.1. The effective width is calculated by first integrating the longitudinal (S11) membrane stresses at cross-sections along the length of the stiffened element and then dividing the resulting areas by the yield stress of the steel as shown in Figure 7.19. The membrane stresses are the longitudinal (S11) stresses that occur at the midplane of the stiffened element as defined in Figure 7.20.

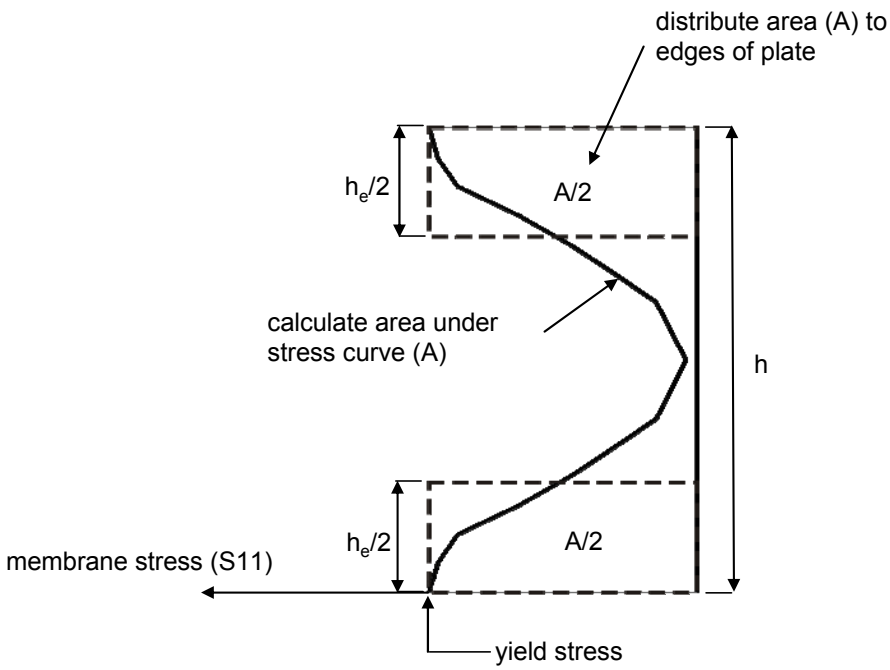

Figure 7.19 Calculation of "effective width" at a cross-section along a stiffened element

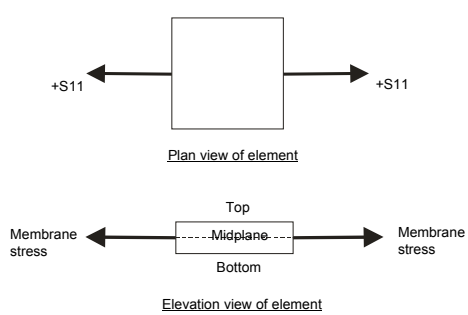

Figure 7.20 Definition of longitudinal (S11) membrane stress

Figure 7.21(a) highlights the variation in membrane longitudinal stress (S11) occurring at the failure load of the stiffened element. The highest stresses accumulate along the edges of the plate and decrease toward the center of the plate. The largest edge stresses occur at the crests of the half-waves where the grey stress contours indicate yielding of the plate. The corresponding effective width is presented in Figure 7.21(b). The maximum effective width of 0.51 h_e/h occurs at the inflection point between half-waves, while the minimum effective width of 0.48 h_e/h occurs at the wave crests. The predicted effective width for this plate using Section B2.1 of the AISI specification is 0.50 h_e/h (AISI-S100 2007).

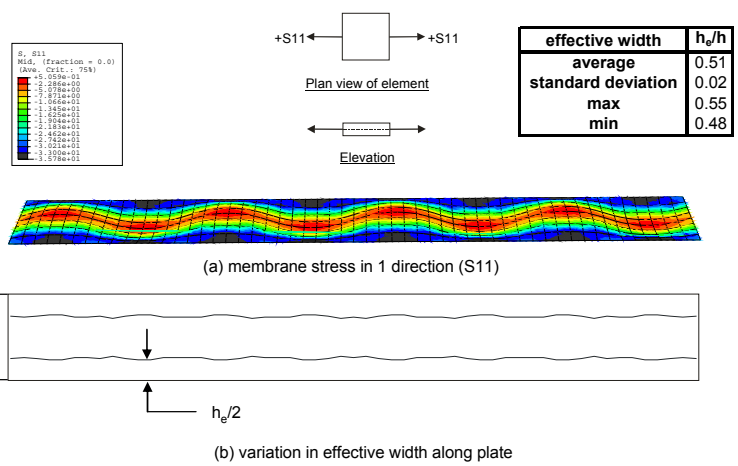

Figure 7.21 (a) longitudinal membrane stresses and (b) effective width of a stiffened element at failure

The failure mode of the stiffened element with the slotted hole is fundamentally different than without the hole. The stresses in Figure 7.22(a) demonstrate that yielding occurs only at the location of the hole when the peak load is reached. Compressive stresses are highest at the edge of the plate and then transition to tensile stresses at the

face of the hole. The effective width of the yielded portion of the plate in Figure 7.22(b) is less than that for the plate without the hole, even with the beneficial tensile stresses at the face. The average effective width is 0.38 h_e/h, which is 25 percent less than that of the stiffened element without the hole. The predicted effective width using Section B2.2 of the AISI Specification is 0.30 h_e/h. The effective widths of the stiffened element with and without a slotted hole are compared together in Figure 7.23.

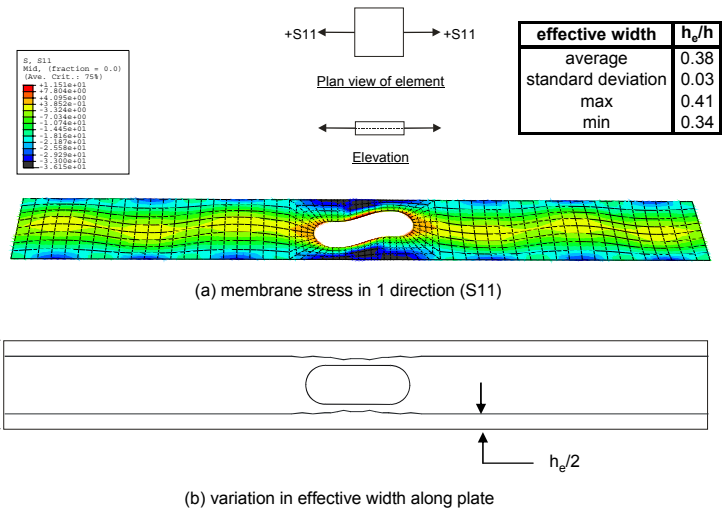

Figure 7.22 (a) longitudinal membrane stresses and (b) effective width of a stiffened element with a slotted hole at failure

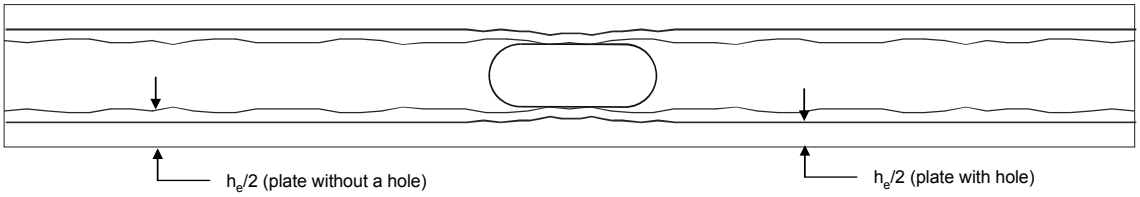

Figure 7.23 Effective width comparison for a plate with and without a slotted hole

The longitudinal stresses (S11) in the top and bottom fibers of the stiffened element at failure are different from the membrane stresses at the midplane, suggesting

that the effective width of a stiffened element actually varies through its thickness. Figure 7.24 and Figure 7.25 provide a comparison of this variation for a stiffened element with and without a slotted hole. It is observed that a plate is more effective on the surface where the out-of-plane deformation causes compression. The effective width is reduced when tensile and compressive stresses negate each other, as shown in the 2D plot of extreme fiber and membrane stresses at a representative cross-section in Figure 7.26.

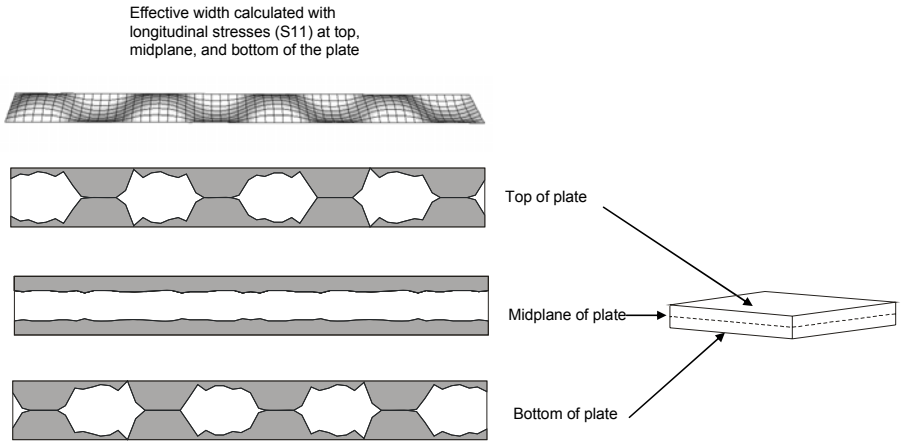

Figure 7.24 Through the thickness variation of effective width of a plate without a hole

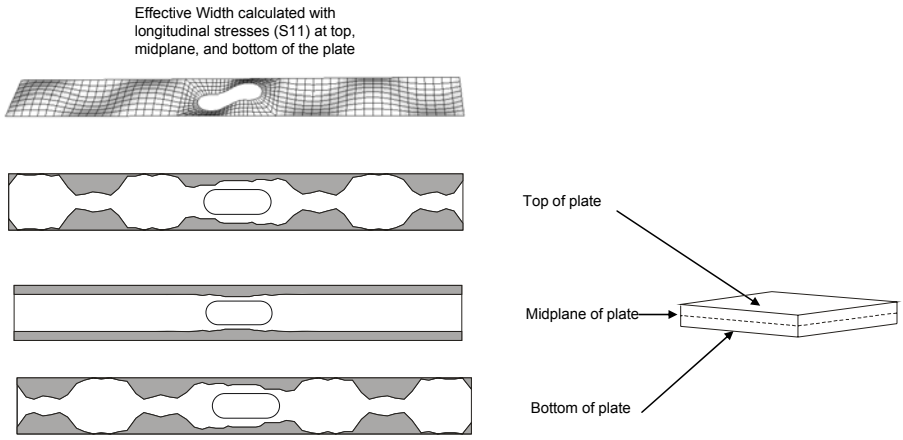

Figure 7.25 Through the thickness variation of effective width of a plate with a slotted hole

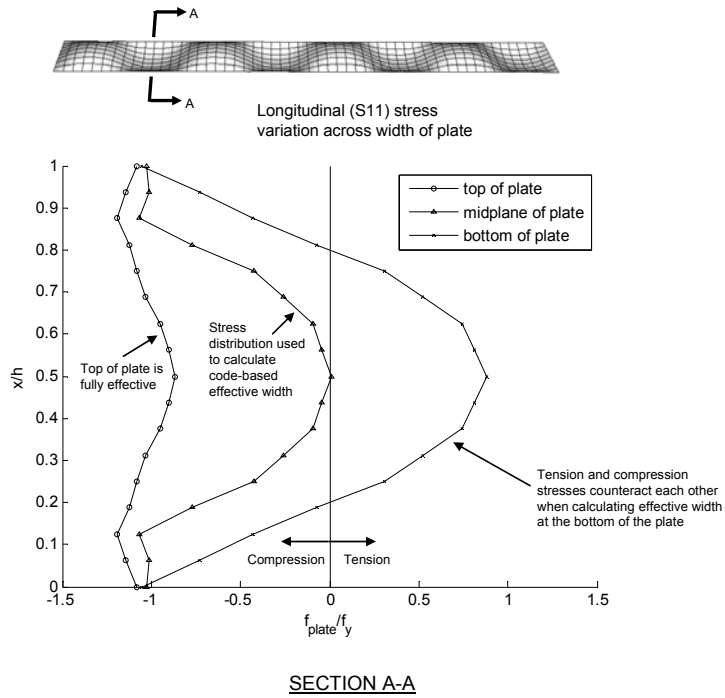

Figure 7.26 Through thickness variation in longitudinal (S11) stresses in a plate at failure

7.2 Nonlinear finite element modeling of columns with holes

A more extensive study of ABAQUS nonlinear finite element capabilities of cold-formed steel columns with holes is now presented. Simulation to collapse of the 24 column experiments described in Chapter 5 is performed, considering solution sensitivity to specific modeling parameters including initial imperfections, residual stresses and the cold-work of forming, nonlinear material modeling, and column boundary conditions. A modeling protocol is developed which produces results consistent with column experiments. This modeling tool is employed to explore the